Journal of Biomechanics 105 (2020) 109792

Contents lists available at ScienceDirect

Journal of Biomechanics

journal homepage: www.elsevier.com/locate/jbiomech
www.JBiomech.com

Incorporating subject-specific geometry to compare metatarsal stress during running with different foot strike patterns

M.A. Ellison [a,*], M. Kenny [a], J. Fulford [b], A. Javadi [c], H.M. Rice [a]

[a] Sport and Health Sciences, University of Exeter, Exeter, UK
[b] NIHR Exeter Clinical Research Facility, University of Exeter Medical School, Exeter, UK
[c] College of Engineering, Mathematics and Physical Sciences, University of Exeter, Exeter, UK

ARTICLE INFO

Article history:
Accepted 4 April 2020

ABSTRACT

Stress fracture of the second metatarsal is a common and problematic injury for runners. The choice of foot strike pattern is known to affect external kinetics and kinematics but its effect on internal loading of the metatarsals is not well understood. Subject-specific models of the second metatarsal can be used to investigate internal loading in a non-invasive manner. This study aimed to compare second metatarsal stress between habitual rearfoot and non-rearfoot strikers during barefoot running, using a novel subject-specific mathematical model, including accurate metatarsal geometry. Synchronised force and kinematic data were collected during barefoot overground running from 20 participants (12 rearfoot strikers). Stresses were calculated at the plantar and dorsal periphery of the midshaft of the metatarsal using a subject-specific beam theory model. Non-rearfoot strikers demonstrated greater external loading, bending moments and compressive forces than rearfoot strikers, but there were no differences in peak stresses between groups. Statistical parametric analysis revealed that non-rearfoot strikers had greater second metatarsal stresses during early stance but that there was no difference in peak stresses. This emphasises the importance of bone geometry when estimating bone stress and supports the suggestion that external forces should not be assumed to be representative of internal loading.

1. Introduction

Running is increasingly popular (van der Worp et al., 2015) and is associated with longevity (Chakravarty et al., 2008; Lee et al., 2014; Schnohr et al., 2013; Wang et al., 2013). However distance running is associated with a high incidence of lower limb injuries (van Gent et al., 2007). One particularly burdensome injury is stress fracture of the metatarsals, which account for 4% of all sporting injuries (Chuckpaiwong et al., 2007). The second metatarsal is one of the most common sites of stress fracture (Bennell et al., 1996; Bennell et al., 1998; Gross and Bunch, 1989; Iwamoto and Takeda, 2003; Milgrom et al., 1985) with 10% of all fractures occurring in the metatarsals and 80–90% of these located in the second and third metatarsals (Chuckpaiwong et al., 2007).

Bones are repeatedly loaded during running and this can lead to the accumulation of microdamage. Microdamage accumulation and its repair is a normal and healthy response to loading, and given enough time will result in the bone becoming more resistant to the loading applied. However, microdamage accumulation alters the properties of bone (Burr et al., 1998) and can increase its susceptibility to stress fracture (Burr, 2011). Metatarsal stress fractures are thought to develop due to cyclic overloading with an intermediate remodelling process, which initially weakens the bone prior to increasing strength (Martin et al., 2015). Without sufficient recovery, further loading can lead to excessive microdamage accumulation (Milgrom et al., 2002; Schaffler and Jepsen, 2000) and increased risk of stress fracture.

Runners can be categorised by their foot strike pattern (Nunns et al., 2013). Most commonly runners land on their heel (rearfoot strike) (de Almeida et al., 2015). This is associated with an early impact peak in the vertical ground reaction force time history and high vertical force loading rates (Lieberman et al., 2010). Conversely, those who do not rearfoot strike display a less distinct impact peak and the vertical force loading rates are typically lower than for a rearfoot striker (Ahn et al., 2014; Lieberman et al., 2010). There has been much discussion about the merits and shortcomings of each foot strike pattern, which is confounded when the influence of footwear is considered. Running in a minimalist shoe

* Corresponding author at: Sport and Health Science, Richards Building, St Luke's Campus, Heavitree Road, Exeter EX1 2LU, UK.
E-mail address: Me351@exeter.ac.uk (M.A. Ellison).

https://doi.org/10.1016/j.jbiomech.2020.109792
0021-9290/

tends to result in a more anterior initial foot contact, resulting in increased loading at the metatarsal phalangeal joint (Firminger and Edwards, 2016) - a potential mechanism for increased stress fracture risk. Metatarsal stress fractures have also been reported when converting from standard running shoes to minimalist shoes (Cauthon et al., 2013, Salzler et al., 2012). However, it is not clear if this was influenced by the effect of the footwear per se or an accompanying change in foot strike. Estimates of metatarsal loading when running with different foot strikes is required to further understand the potential mechanisms for stress fracture.

Efforts to estimate internal bone loading have included direct measurement techniques and mathematical modelling. Direct measurement of bone strain using bone staple strain gauges (Arndt et al., 2002, Milgrom et al., 2002) is invasive, making this impractical for applied research questions due to the limited participant numbers. Mathematical models ranging from simple beam theory (Gross and Bunch, 1989; Nunns et al., 2017; Stokes et al., 1979) to more computationally expensive finite element simulations (Firminger et al., 2017; Li et al., 2017) are a viable alternative and have been used to estimate internal forces acting on the metatarsals during both running and walking. Previously, beam theory has provided valuable insight into potential mechanisms for second metatarsal stress fracture (Gross and Bunch, 1989). This previous research modelled the metatarsal as a hollow elliptical beam and concluded that more accurate, subject-specific bone geometry is required to improve understanding of stress fracture risk.

The aim of this study was to quantify the forces and stresses acting on the second metatarsal during barefoot running, using a subject-specific mathematical model, including accurate metatarsal geometry. Further, this model was used to compare metatarsal loading in rearfoot (RF) and non-rearfoot (NRF) strikers during running. It was hypothesised that NRF strikers would experience greater peak internal second metatarsal loading than RF strikers.

2. Methods

2.1. Participants

20 injury-free participants who described themselves as experienced at running and who were currently participating in running activity >3 times per week and >150 mins per week were recruited. Participants reported no current injuries affecting their running and no lower limb injuries that prevented their normal training within the last year. Eligible participants provided written informed consent. The study was approved by the Sport and Health Sciences Ethics Committee, University of Exeter. Sample size was estimated using G*Power (Faul et al., 2007). Peak pressures under the central forefoot in RF and NRF strikers during running in minimalist shoes were used to determine effect size (Kernozek et al., 2014) as this is an important input variable into the stress model. 12 participants was sufficient based on an alpha of 0.05 and power of 95%. A more conservative sample size of 20 was recruited to account for the subject-specific approach that was expected to increase between-participant variability. Prior to the full running protocol, foot strike was assessed in participants' own running shoes during running over a pressure plate. Participants were not informed of their foot strike pattern. This was later compared to their barefoot trials: two participants displayed a foot strike that was consistently more anterior when barefoot than shod, and these participants were included in the NRF group; two further participants displayed a combination of foot strikes during barefoot running, in which case additional trials were collected such that a complete set matching the shod trial were obtained. RF strikers were classified according to the methods of Cavanagh and Lafortune (1980) (N = 12; 7 Female; age 28 ± 11 years; mass 62.6 ± 10.4 kg; height 1.65 ± 0.07 m); whilst NRF strikers were those with a more anterior foot strike (N = 8; 3 Female; age 20 ± 3 years; mass 72.3 ± 12.3 kg; height 1.73 ± 0.09 m).

3. MR imaging

To determine metatarsal geometry, magnetic resonance (MR) images were collected from each participant whilst lying supine within a 1.5 T superconducting whole body scanner (Gyroscan Intera, Philips, The Netherlands). The second metatarsal was identified via palpation and marked with a fish oil capsule. The unloaded foot was placed against a flat vertical barrier within a quadrature head coil to minimize movement and ensure a consistent foot position. Stacks of triaxial MR images covering the whole of the foot and centred around the second metatarsal were acquired. A T1 weighted (repetition time 20 ms, echo time 4.0 ms, flip angle 50^0) 3D gradient echo sequence was utilised with an in-plane resolution of 0.3 × 0.3 mm and slice thickness of 0.7 mm. Depending on the imaging orientation, 60–160 slices within a stack were required for full coverage.

4. Running protocol

Height and mass were measured whilst participants wore their own running kit. Synchronised kinematic, kinetic and plantar pressure data were collected during barefoot running at 3.6 ms^{-1} using four CX1 units (Codamotion, Charnwood Dynamics Ltd., U.K.) with an integrated force plate (1000 Hz) (AMTI, MA, USA). 19 markers (200 Hz) represented bony landmarks of the foot and shank, similar to the Oxford Foot Model (Carson et al., 2001).

A separate plantar pressure plate (RSscan 0.5 m Hi-End Footscan, Belgium) was placed over the force plate such that the pressure plate was entirely within the boundaries of the force plate. This was positioned flush with a runway comprised of EVA foam - a contact surface intended to represent a shoe midsole. Pressure data were collected at 200 Hz using Footscan software (RSscan Gait v7). An opportunity to warm up was provided and familiarisation trials were completed until the participant was comfortable running at the desired speed. Speed was monitored using light gates (WITTY system, Microgate, Bolzano, Italy). The experimental protocol involved running at a constant speed with a right foot contact within the pressure plate boundaries. A trial was successful when the right foot contacted the pressure plate, speed was 3.6 ms^{-1} (±5%), markers remained visible during foot contact and the investigator observed no unusual movement. Ten successful trials were recorded per participant.

4.1. Stress model

The forces acting on the second metatarsal were estimated using a model similar to Stokes et al. (1979) and Gross and Bunch (1989), with stress calculated at the upper and lower surfaces of the bone at the midpoint of the shaft, using a similar approach to that of Meardon and Derrick (2014).

Fig. 1 shows the forces considered in the model. Assumptions in the model are similar to Stokes et al. (1979) with the following alterations and additions:

1. Flexor muscle forces are represented by a long and short plantar tendon with equal load distribution between them
2. Forces and kinematics in the mediolateral direction are negligible
3. The external forces act at points underneath the distal metatarsal head and toe
4. The masses of the segments are negligible

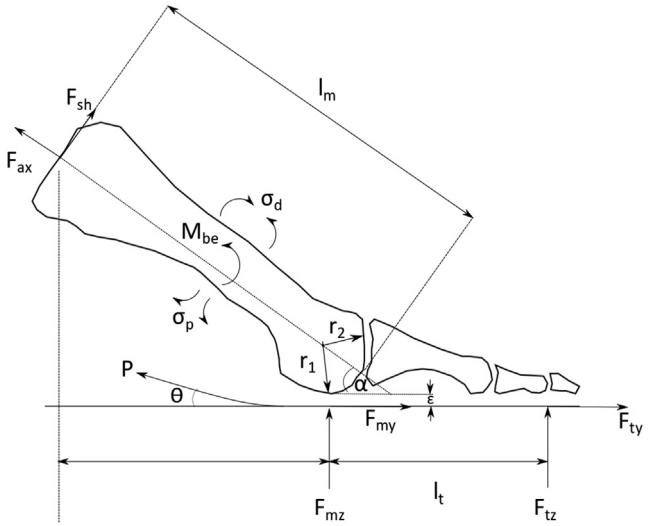

Fig. 1. Forces and dimensions considered in the mathematical model of the second metatarsal and toe. Note: l_m represents metatarsal length, l_t represents toe length, r_1 and r_2 represent the lower and upper radii of the metatarsal head, α represents the angle between the metatarsal and the horizontal, P represents the forces due to the flexor muscles, θ is the angle of plantar tendon action, F_{ax} represents the axial compression force, F_{sh} represents the shear force, M_{be} represents the midshaft bending moments, σ_d and σ_s represent the dorsal and plantar midshaft stresses and ε represents the distance from the lower surface of the metatarsal head to the plantar tendon.

5. The toe segment is parallel to the ground during ground contact

In an adaptation of an earlier approach (Stokes et al., 1979), the combined force due to the long and short plantar tendons was represented by a single force acting in the direction of the midpoint between the two tendons. The angle between tendons (β) was taken to be 10° (Jacob, 2001) thus the angle of plantar tendon action (θ) can be calculated using Eq. (1), with definitions outlined in Fig. 1.

$$\theta = \alpha - \frac{\beta}{2} \tag{1}$$

First the toe is considered in isolation (Fig. 2). The moments acting about the MTP joint are equal to $F_{tz}l_t$. Assuming these moments are attributed to the muscular forces acting at a distance $r_1 + \varepsilon$ from the joint centre gives Eq. (2) where the length ε was the distance from the inferior metatarsal head to the beginning of the fatty tissue under the head.

$$F_{tz}l_t = P(\varepsilon + r_1) \tag{2}$$

In equilibrium the sum of linear forces equate to zero, giving Eq.s 3 and 4. From these, joint reaction forces and plantar tendons forces (P) can be calculated.

$$F_{tz}+F_{jz} + P\sin\theta = 0 \tag{3}$$

$$F_{ty}+F_{jy} - P\cos\theta = 0 \tag{4}$$

Now the metatarsal can be considered (Fig. 3). Resolving forces axially and perpendicularly gives Eq.s 5 and 6. The bending moment at midshaft can be calculated using Eq. (7).

$$F_{ax} = F_{mz}\sin\alpha - F_{my}\cos\alpha+F_{jy}\cos\alpha - F_{jz}\sin \tag{5}$$

$$F_{sh} = F_{mz}\cos\alpha+F_{my}\sin\alpha - F_{jz}\cos\alpha - F_{jy}\sin\alpha \tag{6}$$

$$M_{be} = \left(\frac{l_m - r_2}{2}\right)(F_{mz}\cos\alpha+F_{my}\sin\alpha - F_{jz}\cos\alpha - F_{jy}\sin\alpha) \tag{7}$$

Lastly, stress can be calculated using these derived forces and bending moments, and the cross-sectional geometry of the metatarsal at midshaft.

Axially, the stress is given by Eq. (8), and bending stress is calculated using Eq. (9).

$$\sigma_{ax}=\frac{F_{ax}}{CSA} \tag{8}$$

Eq. (8): Axial stress calculation where CSA represents the cross-sectional area

$$\sigma_{be}=\frac{M_{be}r}{I} \tag{9}$$

Eq. (9): Bending stress calculation where r represents the radial distance from the centre of the bone to the surface, I represents the area moment of inertia about the horizontal axis of the bone cross-section.

Finally, the midshaft stresses at the dorsal and plantar bony surfaces can be calculated using Eq. (10).

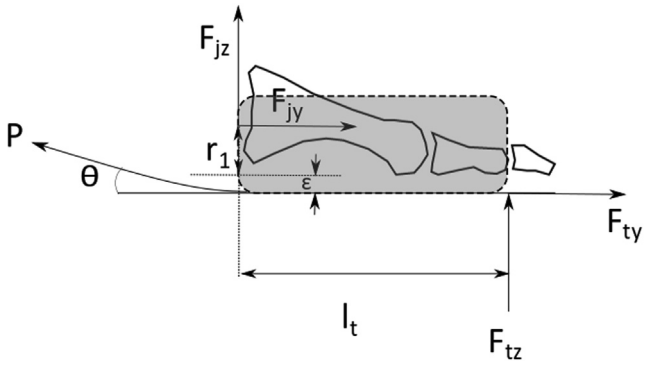

Fig. 2. Free body diagram (grey rectangle) for the toe – F_{tz} and F_{ty} represent the vertical and horizontal ground reaction forces acting under the toe, F_{jz} and F_{jy} represent the vertical and horizontal joint reaction forces at the MTP joint.

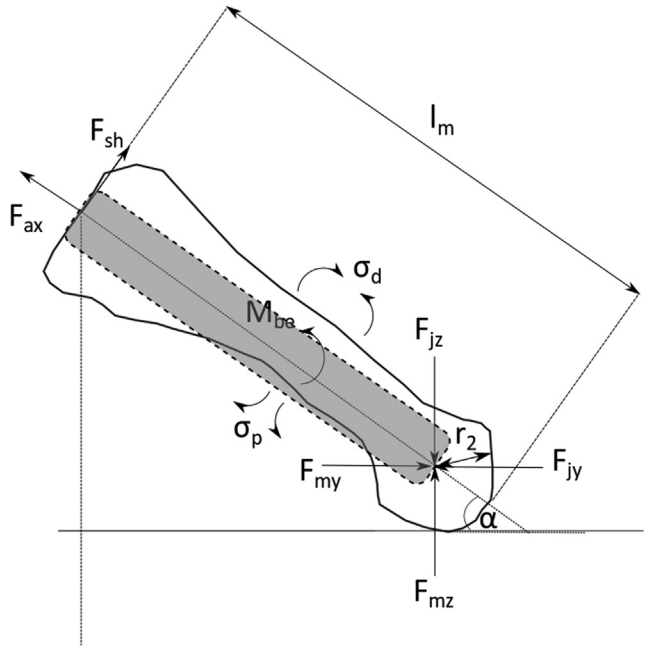

Fig. 3. Free body diagram (grey rectangle) for the metatarsal: F_{mz} and F_{my} represent the vertical and horizontal ground reaction forces acting under the second metatarsal head.

$$\sigma_d = \sigma_{ax} + \sigma_{be}$$
$$\sigma_p = \sigma_{ax} - \sigma_{be} \quad (10)$$

Eq. (10): Normal stress acting on the upper and lower surface of the midshaft, d and p represent dorsal and plantar surfaces, σ_{ax} represents axial stress and σ_{be} represents bending stress.

4.2. Data analysis

The procedure for pressure analysis was taken from Rice et al. (2013) and analysis was performed using RSscan Footscan Gait v7. To obtain estimated ground reaction forces under the second metatarsal head and toe, the plantar pressure in each cell under the metatarsal head and second toe was summed and calculated as a percentage of the pressure across all cells in that frame of stance. Vertical and anterior-posterior ground reaction forces measured using the force plate were scaled by this percentage. This was repeated for each frame of stance. Length l_t was measured from the head of the metatarsal to the point of toe contact with the ground using a flat metal rule during standing. Angle α was the sagittal plane vector angle between the proximal and distal second metatarsal markers and the ground during stance.

The simplified bone geometry for the model was calculated using ImageJ (1.50i, National Institutes of Health, U.S.A.). The radii r_1 and r_2 were calculated using a circle fitting function from an image of the centre of the bone in the sagittal plane, ensuring the distal epiphysis was completely visible. Metatarsal length, l_m, was calculated in the sagittal plane on three consecutive slices in which the bone was completely in view - the mean was obtained.

Cross-sectional information was calculated using an automated custom Matlab script (Kenny et al., 2019). The cross-section image was imported and the brightness adjusted to make the cortical and trabecular bone areas more distinct from the background. A canny edge detection algorithm identified the edges of the bone and the cortical bone was divided into a series of triangles from which the area and area moment of inertia could be calculated (Figs. 4 and 5). Peak values were calculated for F_{mz}, F_{ax}, F_{sh}, M_{be}, σ_p and σ_d and averaged over the ten trials for each participant.

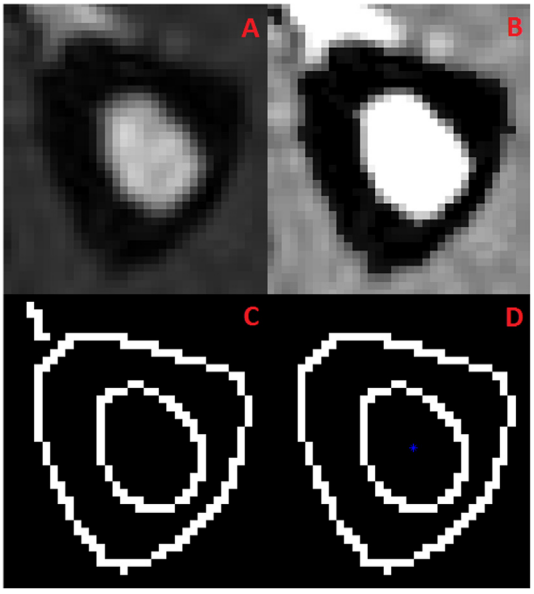

Fig. 4. A: Original image of cross section, B: Image with altered contrast, C: Initial edge detection, D: Final edges with centroid plotted in blue.

4.3. Statistical Analysis

Statistical analysis was conducted in SPSS (Version 24.0, SPSS Inc., Chicago, IL, USA) (discrete variables) and in Matlab using open source statistical parametric mapping (SPM) (http://www.spm1d.org (Pataky et al., 2016)), with a significance level of $P \leq 0.05$. Discrete variables (peak values and bone geometry) were examined using a Shapiro-Wilk test to confirm normality ($P \geq 0.05$). Means were compared using an independent T-Test. Effect sizes were calculated using Cohen's d (Cohen, 1988). Time of peak stress was reported for descriptive purposes.

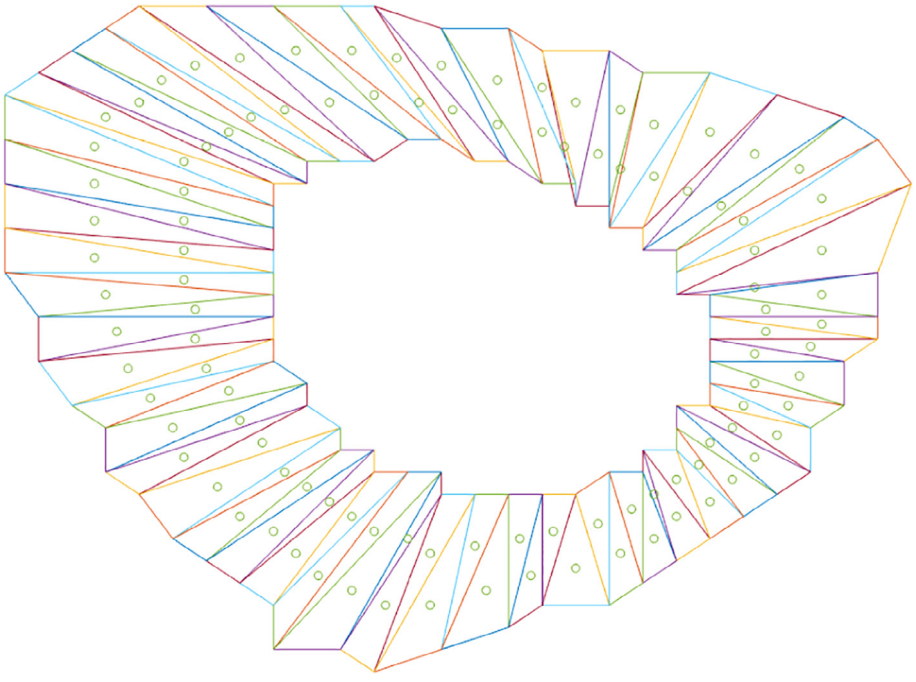

Fig. 5. Outline of cross section divided into triangles, with the centroid of each triangle plotted as circles.

Table 1
Peak forces, peak moments, peak stresses and bone geometry compared between foot strike patterns.

Variable	Mean (SD) RF	NRF	P	d
Peak Dorsal Stress (MPa)	−210.18 (89.66)	−244.73 (36.09)	0.249	0.5
Peak Plantar Stress (MPa)	196.16 (84.62)	223.14 (35.73)	0.341	0.4
Axial Force (N)	**263.60 (89.41)**	**427.79 (63.57)**	**<0.001***	2.1
Shear Force (N)	294.27 (58.80)	342.04 (33.39)	0.053	0.9
Midshaft Bending Moments (N.m)	**9.35 (1.90)**	**11.63 (1.97)**	**0.019***	1.2
vGRF under MT2 Head (N)	**309.01 (63.76)**	**381.98 (57.23)**	**0.018***	1.2
Time of Peak Dorsal Stress (% stance)	58.7 (3.7)	56.6 (3.6)		
Time of Peak Plantar Stress (% stance)	58.5 (3.8)	56.6 (3.4)		
Cross-sectional area (m^2)	3.7×10^{-5} (6.6×10^{-6})	3.8×10^{-5} (5.4×10^{-6})	0.853	0.1
Area moment of inertia (m^4)	2.1×10^{-10} (9.1×10^{-11})	2.1×10^{-10} (7.4×10^{-11})	0.997	0.0
Radial distance from bone centre to surface (m)	3.8×10^{-3} (3.5×10^{-4})	3.9×10^{-3} (2.5×10^{-4})	0.385	0.0

* Significant ($P \leq 0.05$) between groups, negative indicates compressive stress. MT2: second metatarsal.

5. Results

There were no differences in weight or age between groups, however the NRF group was significantly taller than the RF group (1.73 ± 0.09 m vs 1.65 ± 0.07 m, p = 0.049). For all runners, the dorsal surface of the metatarsal was under compression throughout stance whereas the plantar surface was under tension, with similar magnitudes of stress observed on each surface. Average peak compressive stress across the entire group of runners was 224 MPa.

5.1. Discrete analysis

There was greater peak axial force (P = 0.001), peak bending moments (P = 0.019) and peak vGRF under the second metatarsal (P = 0.018) in NRF strikers compared to RF strikers (Table 1). However there was no difference in peak stresses or shear force between foot strikes. Peak dorsal stress values for each individual against body weight are presented in Fig. 6. Peak bending stress contributed 96.3% (±4.39%) to the peak compressive stress on average.

5.2. SPM analysis

NRF strikers showed greater compressive stress on the dorsal surface (Fig. 7A) and greater tensile stress on the plantar surface (Fig. 7B) between 7.3% and 23.4% of stance (P < 0.001). There were no differences in dorsal or plantar stress at the time of peak stress.

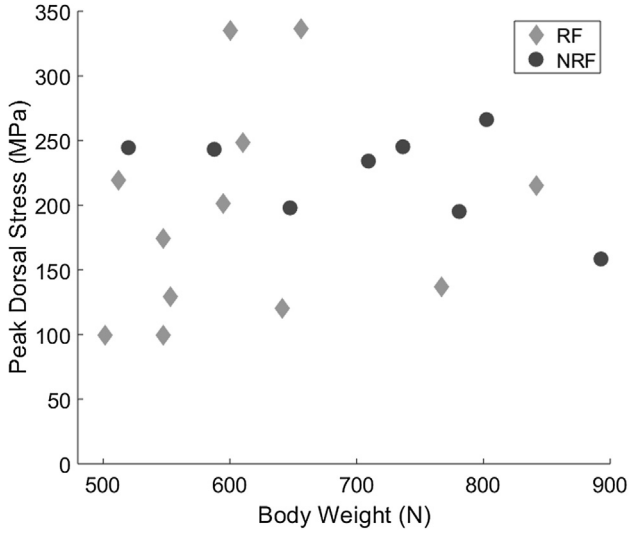

Fig. 6. scatter plot displaying individual peak stress values plotted against body weight for rearfoot (RF) and non-rearfoot (NRF) strikers.

5.3. Discussion

This study developed a novel approach to estimating metatarsal stress during running, adapted from previous beam theory models with the addition of accurate, subject-specific bone geometry and the inclusion of anterior-posterior ground and joint reaction forces. This model was used to compare stresses acting on the second metatarsal during running between runners with different habitual footstrike patterns. The dorsal compression observed throughout stance supports findings from strain gauge data (Arndt et al., 2002) with the exception that a short, initial period of dorsal tension was previously reported. These differences may be due to the location of the strain gauge and its alignment along the length of the bone. Peak pressure under the second metatarsal in the present study (RF: 412 kPa NRF: 572 kPa) was similar in magnitude to that reported by Nunns et al. (2013) (RF: 442 kPa NRF: 464 kPa). Gross and Bunch (1989) used a similar modelling approach during shod running to estimate second metatarsal strain, but modelled the cross-section as a hollow ellipse. Converting their reported strain value to stress using their reported Young's Modulus (17 GPa) reveals stresses of 113 MPa, far lower than in the present study (224 MPa). Both models derived stress from midshaft bending moments which were similar between studies (9.35 N.m for RF strikers in the present study compared with 7.71 N.m reported by Gross and Bunch). This suggests the difference in stress magnitudes between studies is predominantly influenced by the difference in metatarsal geometry. There was a large range of area moment of inertia values in the present study (8.15×10^{-11}-3.83×10^{-10} m^4). When modelling the metatarsals in the present study as a hollow ellipse for comparison with Gross and Bunch the average area moment of inertia was 1.7×10^{-10} m^4, 35 times smaller than the value reported by Gross and Bunch (5.8 e^{-9} m^4), contributing to greater bending stress values despite similar bending moment values. Furthermore, the metatarsal stress reported by Gross and Bunch did not include the contribution due to axial compression.

In vivo strain estimates obtained during barefoot treadmill running (3.1 $m.s^{-1}$) from two participants were 1891 με and 5315 με (Milgrom et al., 2002). Using the same Young's Modulus of 17 GPa, this equates to 32 MPa and 90 MPa respectively, also lower than in the present study. The average peak stress in the present study is higher than reported values for the failure point of cortical bone (e.g. 195 MPa, (Martin et al., 2015)) however, the reported value for the ultimate stress of cortical bone varies greatly depending on the sample site and testing method used (Wolfram and Schwiedrzik, 2016). The disparity between stress values in the pre-

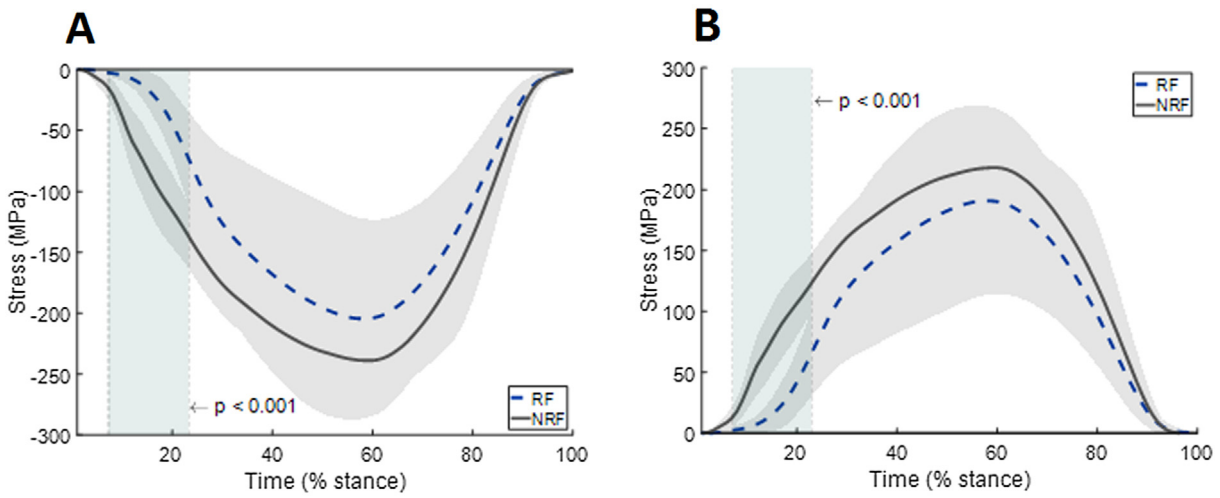

Fig. 7. Comparison of A: dorsal stress between footstrike types, B: plantar stress between footstrike types. Negative values represent compression, Vertical shaded area shows areas of significant differences.

sent study and the literature, including data from strain gauges, suggests that the model presented here is more useful for understanding relative rather than absolute metatarsal loading values.

Compressive and tensile stresses were greater during early stance in NRF than RF strikers according to SPM analyses, but no statistically significant differences were observed at the time of peak stress. Whilst it should be noted that the group representing non-rearfoot strike runners included midfoot, forefoot and toe strikers and these groups have different kinetic and kinematic characteristics (Nunns et al., 2013), the standard deviations of the peak stress values for this group were smaller than for the rearfoot strike group, providing confidence that this grouping is robust when assessing peak second metatarsal stress. Observation of individual peak stress values (Fig. 6) supports this, demonstrating no marked differences in stress magnitudes between groups, influenced in part by a wider range of values in the RF runners. The differences in early stance could be expected based on the more anterior foot contact in NRF than RF strikers, but it is important to note that the peak stresses occurred at the same point during stance in the two foot strike categories. Therefore the significant differences in stress between these groups only occurred in early stance when the stress magnitudes were lower. The magnitude of bone stress is understood to be important when considering risk of stress fracture, but it is not well-established what magnitudes of peak stress may be detrimental. The results from the present study suggest that whilst externally measured forces differ between runners with different foot strike types, this does not equate to a difference in the magnitude of peak metatarsal stress during running, and therefore may not influence the risk of stress fracture via this mechanism. This does not mean that changing from a rearfoot strike to a more anterior foot strike can be recommended as the results from the present study were obtained from runners using their habitual foot strike. Changing foot strike would introduce unaccustomed activity which was not considered in this analysis.

The external forces acting under the metatarsal head were significantly greater in the NRF runners than RF runners and this was also the case for all calculated variables that did not include subject-specific bone geometry, other than shear forces. However the stresses - which are influenced by subject-specific bone geometry - were similar between groups. This supports research suggesting that external loading measures such as plantar pressures and ground reaction forces may not be a valid method of estimating internal loading (Matijevich et al., 2019) as well as research suggesting that geometry is an important determinant of metatarsal stress magnitude (Nunns et al., 2017). The cross-sectional geometry in the present study was obtained using an automated approach and provided a less-simplified estimate of the geometry than used in previous beam theory approaches. The average cross-sectional area of 38 mm^2 in the present study falls between values of 18 mm^2 and 51 mm^2 that have previously been reported in the second metatarsal (Courtney et al., 1997; Marchi, 2005).

The model provides a useful tool for estimating internal metatarsal loading during barefoot running. However, models require assumptions and these introduce limitations. The model did not account for surrounding soft tissues in the foot. This soft tissue cushions and distributes forces, thus the model used may have overestimated stresses. Modelling the interaction of these soft tissues would be beneficial when investigating the forces in the metatarsals during running. Only non-deformable geometry was included and this does not reflect the complex three-dimensional shape of the metatarsal. The use of continuum mechanics such as a finite element model would reduce these limitations. This study assessed metatarsal stress during barefoot running, whereas the majority of runners wear shoes during running. Previous studies have shown that footwear can affect external forces differently depending on foot strike pattern (Rice et al., 2016). Assessment of metatarsal stress during barefoot running removed the confounding influence of footwear but does not truly represent the habitual running condition of the participants.

6. Conclusion

Habitual non-rearfoot strikers experience greater second metatarsal stresses during early stance than habitual rearfoot strikers during barefoot running, but similar peak stresses. This is despite non-rearfoot strikers experiencing greater peak external loading under the metatarsal head, resulting in greater peak bending moments about the midshaft than rearfoot strikers. These findings emphasise the importance of including subject-specific geometry when estimating bone stress and further supports the suggestion that external forces should not be assumed to be representative of internal loading.

Declaration of Competing Interest

The authors declare that they have no known competing financial interests or personal relationships that could have appeared to influence the work reported in this paper.

Acknowledgements

This work was conducted as part of an Engineering and Physical Sciences Research Council, grant number 1772954 funded doctoral training program.

References

Ahn, A.N., Brayton, C., Bhatia, T., Martin, P., 2014. Muscle activity and kinematics of forefoot and rearfoot strike runners. J. Sport Health Sci. 3, 102–112.
Arndt, A., Ekenman, I., Westblad, P., Lundberg, A., 2002. Effects of fatigue and load variation on metatarsal deformation measured in vivo during barefoot walking. J. Biomech. 35, 621–628.
Bennell, K.L., Malcolm, S.A., Brukner, P.D., Green, R.M., Hopper, J.L., Wark, J.D., Ebeling, P.R., 1998. A 12-month prospective study of the relationship between stress fractures and bone turnover in athletes. Calcif. Tissue Int. 63, 80–85.
Bennell, K.L., Malcolm, S.A., Thomas, S.A., Wark, J.D., Brukner, P.D., 1996. The incidence and distribution of stress fractures in competitive track and field athletes. American J. Sports Med. 24, 211–217.
Burr, D., 2011. Why bones bend but don't break. J. Musculoskelet. Neuronal Interact. 4, 270–285.
Burr, D.B., Turner, C.H., Naick, P., Forwood, M.R., Ambrosius, W., Hasan, M.S., Pidaparti, R., 1998. Does microdamage accumulation affect the mechanical properties of bone?. J. Biomech. 31, 337–345.
Carson, M.C., Harrington, M.E., Thompson, N., O'connor, J.J., Theologis, T.N., 2001. Kinematic analysis of a multi-segment foot model for research and clinical applications: a repeatability analysis. J. Biomech. 34, 1299–1307.
Cauthon, D.J., Langer, P., Coniglione, T.C., 2013. Minimalist shoe injuries: three case reports. Foot 23, 100–103.
Cavanagh, P.R., Lafortune, M.A., 1980. Ground reaction forces in distance running. J. Biomech. 13, 397–406.
Chakravarty, E.F., Hubert, H.B., Lingala, V.B., Fries, J.F., 2008. Reduced disability and mortality among aging runners: a 21-year longitudinal study. Arch. Intern. Med. 168, 1638–1646.
Chuckpaiwong, B., Cook, C., Pietrobon, R., Nunley, J.A., 2007. Second metatarsal stress fracture in sport: comparative risk factors between proximal and non-proximal locations. British J. Sports Med. 41, 510–514.
Cohen, J., 1988. The Analysis of Variance. Statistical Power Analysis for the Behavioral Sciences,. Lawrence Erlbaum Associates.
Courtney, A.C., Davis, B.L., Manning, T., Kambic, H.E., 1997. Effects of age, density, and geometry on the bending strength of human metatarsals. Foot Ankle Int. 18, 216–221.
De Almeida, M.O., Saragiotto, B.T., Yamato, T.P., Lopes, A.D., 2015. Is the rearfoot pattern the most frequently foot strike pattern among recreational shod distance runners? Phys. Therapy Sport. 16, 29–33.
Faul, F., Erdfelder, E., Lang, A.-G., Buchner, A., 2007. G*Power 3: A flexible statistical power analysis program for the social, behavioral, and biomedical sciences. Behavior Res. Meth. 39, 175–191.
Firminger, C.R., Edwards, W.B., 2016. The influence of minimalist footwear and stride length reduction on lower-extremity running mechanics and cumulative loading. J. Sci. Med. Sport 19, 975–979.
Firminger, C.R., Fung, A., Loundagin, L.L., Edwards, W.B., 2017. Effects of footwear and stride length on metatarsal strains and failure in running. Clin. Biomech. 49, 8–15.
Gross, T.S., Bunch, R.P., 1989. A mechanical model of metatarsal stress fracture during distance running. Am. J. Sports Med. 17, 669–674.
Iwamoto, J., Takeda, T., 2003. Stress fractures in athletes: review of 196 cases. J Orthop Sci 8, 273–278.
Jacob, H.A., 2001. Forces acting in the forefoot during normal gait–an estimate. Clin. Biomech. (Bristol, Avon) 16, 783–792.
Kenny, M., Ellison, M., Rice, H., 2019. Matlab code to digitise MR bone images and calculate properties of shape: cross-sectional area, area moment of inertia, product moment of area. 1.0 ed. Open Research Exeter: University of Exeter.
Kernozek, T.W., Meardon, S., Vannatta, C.N., 2014. In-Shoe Loading in rearfoot and non-rearfoot strikers during running using minimalist footwear. Int. J. Sports Med. 35, 1112–1117.
Lee, D.-C., Pate, R.R., Lavie, C.J., Sui, X., Church, T.S., Blair, S.N., 2014. Leisure-time running reduces all-cause and cardiovascular mortality risk. J. Am. Coll. Cardiol. 64, 472–481.
Li, S., Zhang, Y., Gu, Y., Ren, J., 2017. Stress distribution of metatarsals during forefoot strike versus rearfoot strike: A finite element study. Comput. Biol. Med. 91, 38–46.
Lieberman, D.E., Venkadesan, M., Werbel, W.A., Daoud, A.I., D'andrea, S., Davis, I.S., Mang'eni, R.O., Pitsiladis, Y., 2010. Foot strike patterns and collision forces in habitually barefoot versus shod runners. Nature 463, 531.
Marchi, D., 2005. The cross-sectional geometry of the hand and foot bones of the Hominoidea and its relationship to locomotor behavior. J. Hum. Evol. 49, 743–761.
Martin, R.B., Burr, D.B., Sharkey, N.A., Fyhrie, D.P., 2015. Skeletal tissue mechanics. Springer, New York.
Matijevich, E.S., Branscombe, L.M., Scott, L.R., Zelik, K.E., 2019. Ground reaction force metrics are not strongly correlated with tibial bone load when running across speeds and slopes: Implications for science, sport and wearable tech. PLoS ONE 14, e0210000.
Meardon, S.A., Derrick, T.R., 2014. Effect of step width manipulation on tibial stress during running. J. Biomech. 47, 2738–2744.
Milgrom, C., Finestone, A., Sharkey, N., Hamel, A., Mandes, V., Burr, D., Arndt, A., Ekenman, I., 2002. Metatarsal strains are sufficient to cause fatigue fracture during cyclic overloading. Foot Ankle Int. 23, 230–235.
Milgrom, C., Giladi, M., Stein, M., Kashtan, H., Margulies, J., Chisin, R., Steinberg, R., Aharonson, Z., 1985. Stress fractures in military recruits. a prospective study showing an unusually high incidence. J. Bone Joint Surgery British 67-B, 732–735.
Nunns, M., House, C., Fallowfield, J., Allsopp, A., Dixon, S., 2013. Biomechanical characteristics of barefoot footstrike modalities. J. Biomech. 46, 2603–2610.
Nunns, M., Stiles, V., Fulford, J., Dixon, S., 2017. Estimated third metatarsal bending stresses are highly susceptible to variations in bone geometry. Footwear Sci., 1–11
Pataky, T.C., Robinson, M.A., Vanrenterghem, J., 2016. Region-of-interest analyses of one-dimensional biomechanical trajectories: bridging 0D and 1D theory, augmenting statistical power. PeerJ 4, e2652.
Rice, H., Nunns, M., House, C., Fallowfield, J., Allsopp, A., Dixon, S., 2013. High medial plantar pressures during barefoot running are associated with increased risk of ankle inversion injury in Royal Marine recruits. Gait Post. 38, 614–618.
Rice, H.M., Jamison, S.T., Davis, I.S., 2016. Footwear matters: influence of footwear and foot strike on load rates during running. Med. Sci. Sports Exerc. 48, 2462–2468.
Salzler, M.J., Bluman, E.M., Noonan, S., Chiodo, C.P., De Asla, R.J., 2012. Injuries observed in minimalist runners. Foot Ankle Int. 33, 262–266.
Schaffler, M.B., Jepsen, K.J., 2000. Fatigue and repair in bone. Int. J. Fatigue 22, 839–846.
Schnohr, P., Marott, J.L., Lange, P., Jensen, G.B., 2013. Longevity in male and female joggers: the copenhagen city heart study. Am. J. Epidemiol. 177, 683–689.
Stokes, I.A., Hutton, W.C., Stott, J.R., 1979. Forces acting on the metatarsals during normal walking. J. Anat. 129, 579–590.
Van Der Worp, M.P., Ten Haaf, D.S.M., Van Cingel, R., De Wijer, A., Nijhuis-Van Der Sanden, M.W.G., Staal, J.B., 2015. Injuries in runners; a systematic review on risk factors and sex differences. PLoS ONE 10, e0114937.
Van Gent, R.N., Siem, D., Van Middelkoop, M., Van Os, A.G., Bierma-Zeinstra, S.M.A., Koes, B.W., 2007. Incidence and determinants of lower extremity running injuries in long distance runners: a systematic review. Br. J. Sports Med. 41, 469–480.
Wang, N., Zhang, X., Xiang, Y.-B., Li, H., Yang, G., Gao, J., Zheng, W., Shu, X.-O., 2013. Associations of Tai Chi, walking, and jogging with mortality in Chinese men. Am. J. Epidemiol. 178, 791–796.
Wolfram, Uwe, Schwiedrzik, Jakob, 2016. Post-yield and failure properties of cortical bone. BoneKEy Rep. 5. https://doi.org/10.1038/bonekey.2016.60.